Defective signal transduction in B lymphocytes lacking presenilin proteins

Tomohito Yagi*†, Cosmas Giallourakis‡, Subhasis Mohanty*, Christina Scheidig*, Jie Shen§, Hui Zheng¶, Ramnik J. Xavier‡‖**, and Albert C. Shaw*††

*Section of Infectious Diseases, Department of Internal Medicine, Yale University School of Medicine, New Haven, CT 06520; ‡Gastrointestinal Unit and ‖Center for Computational and Integrative Biology, Massachusetts General Hospital and Harvard Medical School, Boston, MA 02115; §Center for Neurologic Diseases, Brigham and Women's Hospital, Boston, MA 02115; and ¶Huffington Center on Aging, Baylor College of Medicine, Houston, TX 77030

Edited by Adrian T. Ting, Mount Sinai School of Medicine, and accepted by the Editorial Board November 17, 2007 (received for review August 16, 2007)

The mammalian presenilin (PS) proteins mediate the posttranslational cleavage of several protein substrates, including amyloid precursor protein, Notch family members, and CD44, but they have also been suggested to function in diverse cellular processes, including calcium-dependent signaling and apoptosis. We carried out an integrative computational study of multiple genomic datasets, including RNA expression, protein interaction, and pathway analyses, which implicated PS proteins in Toll-like receptor signaling. To test these computational predictions, we analyzed mice carrying a conditional allele of *PS1* and a germ line-inactivating allele of *PS2*, together with Cre site-specific recombinase expression under the influence of CD19 control sequences. Notably, B cells deficient in both PS1 and PS2 function have an unexpected and substantial deficit in both lipopolysaccharide and B cell antigen receptor-induced proliferation and signal transduction events, including a defect in anti-IgM-mediated calcium flux. Taken together, these results demonstrate a fundamental and unanticipated role for PS proteins in B cell function and emphasize the potency of (systems level) integrative analysis of whole-genome datasets in identifying novel biologic signal transduction relationships. Our findings also suggest that pharmacologic inhibition of PS for the treatment of conditions such as Alzheimer's disease may have potential consequences for immune system function.

B cell | computational biology | gene targeting | Toll-like receptor | B cell antigen receptor (BCR)

The mammalian presenilin (PS) proteins PS1 and PS2 are members of the family of intramembrane-cleaving proteases (I-CLiPs) that mediate the regulated proteolysis of a diverse group of substrates including Notch family members, CD44, amyloid precursor protein and the N- and E-cadherins (1, 2). In addition, PS proteins have been implicated in several additional cellular processes, including calcium-dependent signaling (3–5). However, elucidation of PS functions in the immune system has been complicated by the perinatal lethality resulting from germ line inactivation of *PS1* and the embryonic lethality of mice carrying germ line deletions in both *PS1* and *PS2* (6–8). Analyses of PS2-deficient mice with reduced PS1 expression ($PS1^{+/-}$ $PS2^{-/-}$) revealed age-associated myeloproliferative or autoimmune disease but no reported effects on lymphocyte development and function (9, 10). We carried out a systems level integrative analysis based on computationally mining and integrating multiple genomic datasets including cap analysis gene expression (CAGE) and mRNA expression profiling, pathway analysis, and protein interaction maps that implicated PS proteins in signal transduction in the immune system, and we tested these predictions in murine B cells deficient in both PS1 and PS2.

Results

Integrative Computational Analysis of Whole-Genome Datasets Reveals a Role for PS Proteins in Toll-like Receptor (TLR) Signaling. The development of integrative tools to analyze genomic datasets in the context of modular concepts (modular concept maps) or gene sets (gene set enrichment analysis) that share a common biological theme has facilitated insights into processes dysregulated in cancer and diabetes (11, 12). In parallel, we have developed an analytical framework termed immune network maps (INPs) that integrates multiple data types to generate a network of relationships relevant to the immune system embedded in large-scale public genomic datasets (C.G. and R.J.X., unpublished data). We applied a general model of this approach to assist in the identification of pathway(s) relevant to PS proteins in the immune system.

We used a public compendium of mRNA profiles derived from exonic splicing arrays across 52 normal human tissue/cells types, identifying the expression of PS proteins in tissues of the immune system, including bone marrow, tonsil, and spleen (Fig. 1*A*) (13). These results suggested that PS2 expression was overrepresented in the immune system and were further corroborated by analyzing the normalized expression patterns of PS1 and PS2 in murine B cell populations (14) [supporting information (SI) Fig. 6]. To place PS expression in a signaling pathway context, we next analyzed clustering results from the RIKEN CAGE tags, which measure murine expression levels of transcription start sites by using concatenated DNA tags from the initial ≈20 nt of transcript 5′ ends. Hierarchical clustering of the normalized expression values of $>1 \times 10^6$ CAGE tags, representing the promoter activities of associated genes across 23 different tissues/cells under various conditions including LPS stimulation revealed 70 expression supermodules (15). Among these modules was a set of 746 coregulated genes (module 64) preferentially expressed in cells of the immune system, which also harbored known microRNAs (e.g., miR-155 and miR-223) [Fig. 1*B* (for full gene annotation, see SI Table 1)]. This 746-gene set contained genes encoding proteins known to be important in innate immune signaling such as Tlr4, Nod2, Ncf1, and Myd88, as well as novel genes that unexpectedly included PS2. Because coregulation of microarray mRNA profiles often implies that members of a coregulated gene set share function(s), this

Author contributions: T.Y., C.G., S.M., R.J.X., and A.C.S. designed research; T.Y., C.G., S.M., C.S., R.J.X., and A.C.S. performed research; J.S. and H.Z. contributed new reagents/analytic tools; T.Y., C.G., S.M., C.S., R.J.X., and A.C.S. analyzed data; and T.Y., C.G., R.J.X., and A.C.S. wrote the paper.

The authors declare no conflict of interest.

This article is a PNAS Direct Submission. A.T.T. is a guest editor invited by the Editorial Board.

†Present address: Division of Genomic Medical Sciences, Department of Molecular Medical Sciences, Kyoto Prefectural University of Medicine, Kyoto 602-8566, Japan.

**To whom correspondence may be addressed at: Center for Computational and Integrative Biology, Massachusetts General Hospital, Boston, MA 02114. E-mail: xavier@molbio.mgh.harvard.edu.

††To whom correspondence may be addressed at: Yale University School of Medicine, Section of Infectious Diseases, 300 Cedar Street, Box 208022, New Haven, CT 06520. E-mail: albert.shaw@yale.edu.

This article contains supporting information online at www.pnas.org/cgi/content/full/0707755105/DC1.

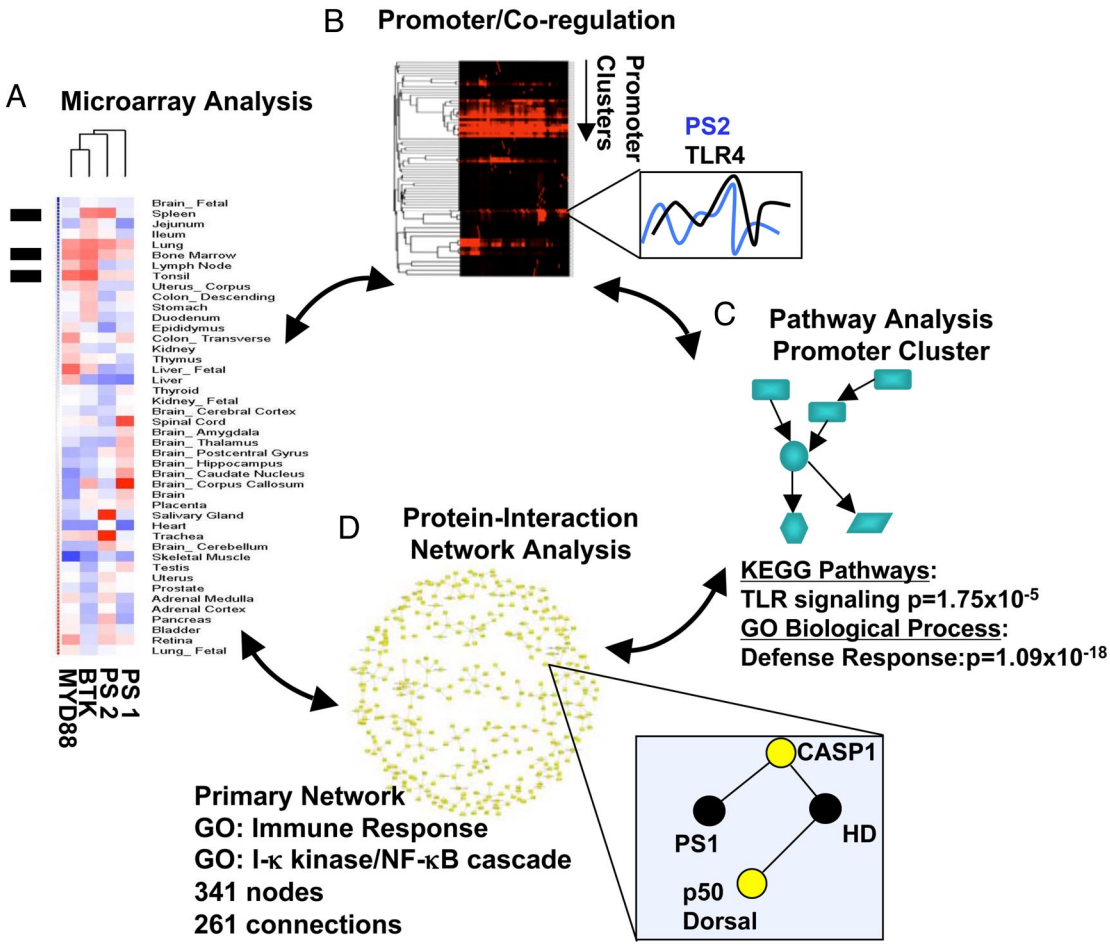

Fig. 1. Computation framework used to identify PSs as a potential functional component of TLR signaling pathways. (*A*) Hierarchical clustering of a subset of tissues from the Rosetta dataset showing expression of PS1, PS2, MyD88, and BTK in immune subcompartments (black bars). (*B*) Expression clustering from CAGE data (http://gerg01.gsc.riken.jp/expr_tree/mm5) representing promoter usage across 23 tissues with a cluster ID = 64 (n = 746 genes) derived from immune cells (including macrophages stimulated with LPS) and schematic depiction of coregulation of TLR4 with PS2. (*C*) Statistical analysis of KEGG pathways and GO ontologies shows that the CAGE cluster of 746 genes includes TLR4 and PS2 and is statistically enriched for pathways such as TLR signaling ($P = 1.75 \times 10^{-5}$) and GO biological processes (e.g., defense response $P = 1.09 \times 10^{-18}$). (*D*) Immune response and NF-κB pathway protein–protein interaction network connected by edges. The interactions are derived from the BIND database and visualized in Cytoscape. An illustrated example of first-order expansion of the base network identifies PS1 as an interactor with caspase-1 (CASP1) and HD (Huntingtin) interactions with CASP1 and p50.

746-gene set based on CAGE clustering suggested a potential role for presenilin in TLR signaling (16–18).

To ascertain rigorously whether the immune CAGE module was statistically enriched for specific processes or pathways in an unbiased manner, we analyzed the annotation of the 746-gene module in Gene Ontology (GO) biological process categories and participation in the *Kyoto Encyclopedia of Genes and Genomes* (KEGG) pathways. Importantly, the CAGE signature exhibited significant enrichment in a number of GO biological processes (e.g., defense response $P = 1.09 \times 10^{-18}$) and KEGG pathways (TLR signaling $P = 1.75 \times 10^{-5}$; Fischer's exact test, Bonferroni-corrected), suggesting that coexpressed genes within this module, including the PS, are functionally related to TLR signaling pathways (Fig. 1*C*) (for results of full analyses of GO biological processes and KEGG pathways, see SI Tables 2 and 3) (19); consistent with this hypothesis, the analysis of 10 different CAGE promoter expression clusters failed to reveal additional modules enriched in TLR signaling pathway(s). We also projected the human orthologs of these genes (n = 697) onto an independent set of microarray expression profiles composed of 79 human tissues/cell types. Using a Wilcoxon rank sum statistic, we observed that a significant fraction of these human orthologs (58.5%) was also expressed preferentially in the immune system (20) ($P < 0.05$; SI Fig. 7 and SI Tables 1 and 4), thereby providing cross-validation for the murine 746-gene module harboring the TLR CAGE signature.

As an additional computational strategy to elucidate potential connections of PS with immune signaling proteins, we created an human immune protein–protein interaction network based on GO annotation by requiring that every protein in the network be annotated as either immune response (GO:0006955) or NF-κB cascade (GO:0007249) and harnessing the BIND database, which includes protein–protein interactions from the literature and multiple large-scale interactomes. This approach yielded an immune-anchored network consisting of 341 nodes with 261 connections (Fig. 1*D* and SI Table 5). Next, we extended this NF-κB/immune response network by one degree of freedom, identifying proteins that interacted with the immune/NF-κB node without any GO annotation restrictions, allowing us to capture proteins not annotated as immune-related but that via their protein–protein interactions may have undiscovered roles in immune processes. Notably, this analysis revealed described

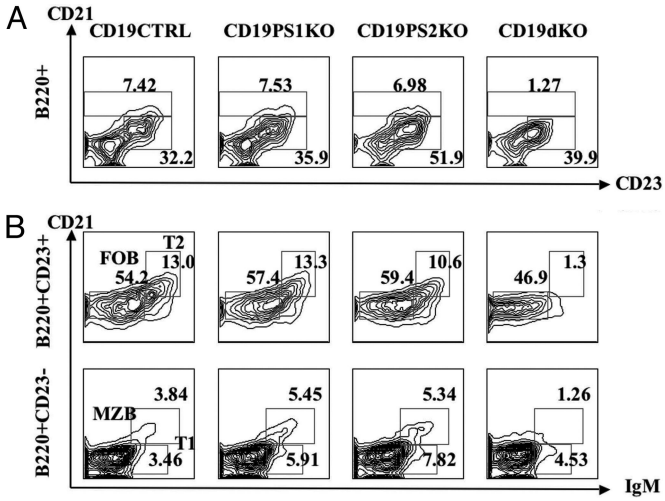

Fig. 2. Defects in mature B cell development in the absence of PS proteins. (*A*) Flow cytometry profiles of CD21 and CD23 expression, gated on $B220^+$ splenocytes. The $B220^+CD21^+CD23^{lo}$ marginal zone and $B220^+CD21^+CD23^+$ splenic follicular B cell populations are indicated. (*B*) Flow cytometry profiles of CD21 vs. IgM expression, gated on $CD23^+$ (*Upper*) and $CD23^-$ (*Lower*) splenocytes. The percentages of follicular B (FOB), T1, T2, and marginal zone B (MZB) cell populations are indicated.

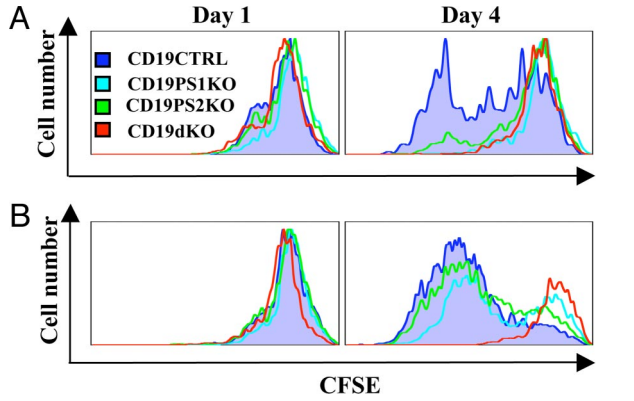

Fig. 3. Decreased proliferation in B cells lacking PS proteins. Flow cytometry profiles of CFSE fluorescence of control, PS1-deficient, PS2-deficient, and PS1/PS2-deficient purified B cells at day 1 and day 4 after stimulation with 5 μg/ml $F(ab')_2$ anti-IgM (*A*) and 20 μg/ml LPS (*B*) are shown. Data are representative of four independent experiments.

interactions in the nervous system of the Huntingtin (HD) protein with caspase-1 (21, 22) and with p50 (23) (Fig. 1*D*) in the context of potential function in the immune system. Our analysis also revealed a connection of PS1 and caspase-1 (GO:0007249), a central component of the inflammasome activated by innate immune signaling (24). Taken together, in this system, the level integration of orthogonal data ranging from CAGE coregulation to protein–protein interaction network with pathway analysis indicates a role for PS in TLR-mediated signaling.

Generation of B Cells Deficient in PS1 and PS2. Testing these predictions was complicated by the perinatal lethality observed upon germ line targeting of PS1 and the embryonic lethal phenotype observed in germ line PS1/PS2 double knockouts (6–8). Consequently, we used a conditional allele of *PS1* (25) crossed into a germ line $PS2^{-/-}$ background (6), with PS1 inactivation in the B cell lineage resulting from the expression of the Cre recombinase under the control of CD19 control sequences (26). We used semiquantitative PCR on magnetic bead-purified splenic B cells from such CD19-Cre/$PS1^{flox/flox}$/$PS2^{-/-}$ mice and observed 75–85% deletion of the conditional *PS1* allele (SI Fig. 8).

Perturbed Development and an Unanticipated Defect in Mitogenic Proliferation in PS-Deficient B Cells. In B cells deficient in either PS1 or PS2, development appeared unperturbed; however, in CD19-Cre/$PS1^{flox/flox}$/$PS2^{-/-}$ mice lacking both PS1 and PS2 function in B cells, development of the marginal zone and T2 transitional B cell compartments in the spleen was selectively impaired relative to follicular and T1 cell populations (Fig. 2 and SI Fig. 9). We did not observe altered development of B cell precursors in the bone marrow, although the extent of PS1 deletion in this compartment was significantly lower (≈40–50%) than in B cells from peripheral lymphoid tissues (data not shown).

We then assessed functional properties of B cells lacking PS1 and PS2 function. We measured the dilution of 5- or 6-(*N*-succinimidyloxycarbonyl)-3′,6′-*O*,*O*′-diacetylfluorescein (CFSE) fluorescence as an indicator of cell division after treatment of B cells from PS1-deficient, PS2-deficient, or both PS1- and PS2-deficient backgrounds with either anti-IgM antibodies or with LPS. After anti-IgM treatment, proliferation was decreased relative to control in PS1-deficient and PS2-deficient B cells but was markedly defective in PS1/PS2-double-deficient B cells. Upon LPS treatment, we observed preserved but decreased proliferation relative to control for both PS1-deficient and PS2-deficient B cells but absent cell division in B cells lacking both PS1 and PS2 (Fig. 3). Taken together, these data suggest that PS function is necessary for B cell proliferation to mitogenic stimuli.

Defective B Cell Antigen Receptor (BCR)- and TLR4-Mediated Signaling in PS-Deficient B Cells. The defect in proliferation mediated by anti-IgM or LPS suggested that signal transduction events downstream of the BCR or TLR4 were defective in the setting of PS deficiency. Accordingly, we assessed the phosphorylation of the nonreceptor tyrosine kinase Syk after BCR engagement with anti-IgM and of the p38 MAP kinase after LPS stimulation via TLR4 by using antibodies recognizing phosphorylated forms of these kinases. Notably, both Syk and p38 phosphorylation were reduced compared with control in B cells lacking either PS1 or PS2 but were markedly defective in cells lacking both PS1 and PS2 (Fig. 4 *A* and *B*).

To evaluate the basis for the proliferative and signaling defect observed in double-deficient PS1/PS2 B cells, we measured changes in intracellular calcium resulting from anti-IgM treatment. Such calcium flux was diminished relative to control in B cells deficient in either PS1 or PS2 but was markedly affected in cells lacking both PS1 and PS2. Although PS1/PS2-double-deficient B cells have the capacity to increase intracellular calcium, as evidenced by calcium flux observed in response to ionomycin treatment, the ionomycin-mediated increase in intracellular calcium was consistently lower in such cells compared with PS1-deficient, PS2-deficient, or control B cells (Fig. 4*C*).

The disruption in early signal transduction events and impaired proliferation we observed downstream of the BCR and TLR4 led us to evaluate the activation of apoptosis in PS-deficient B cells by detecting caspase activation with a flow cytometry-based assay. We observed increased levels of caspase activation after both LPS and anti-IgM stimulation in cells deficient in either PS1 or PS2, particularly after anti-IgM treatment (Fig. 5). However, increased levels of activated caspases were observed after stimulation with either mitogenic agent in B cells deficient in both PS1 and PS2, suggesting that alterations in B cell activation resulting from PS deficiency result in activation of proapoptotic pathways.

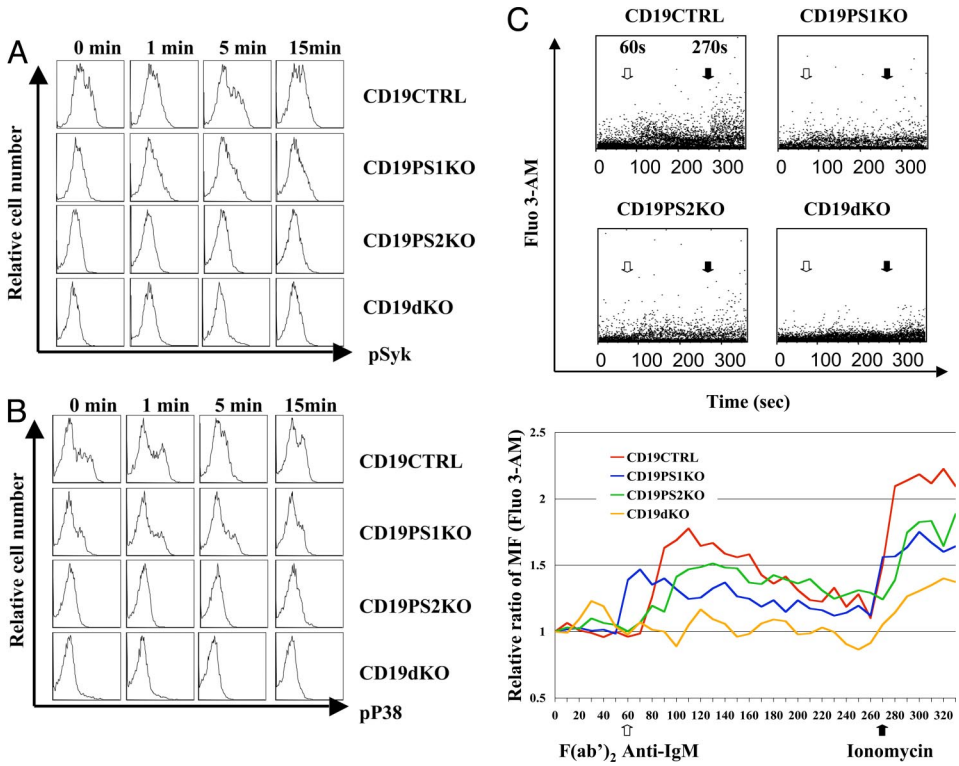

Fig. 4. Defective signal transduction in B cells lacking PS proteins. (*A* and *B*) Flow cytometry histograms of B220$^+$ gated cells from control, PS1-deficient, PS2-deficient, and PS1/PS2-deficient B lineage splenocytes. (*A*) Syk phosphorylation after treatment with 10 μg/ml F(ab′)$_2$ anti-IgM. (*B*) p38 MAPK phosphorylation after treatment with 20 μg/ml LPS. (*C*) Decreased calcium flux in B cells lacking PS proteins. (*Upper*) Flow cytometry plots of Fluo3-AM fluorescence in B220$^+$ gated splenocytes from control, PS1-deficient, PS2-deficient, and PS1/PS2-deficient backgrounds. An identical number of B220$^+$ events was acquired for each panel. (*Lower*) Relative fluorescence of Fluo3-AM plotted as a ratio of mean fluorescence intensity (MFI) to baseline. Open arrows indicate the administration of 10 μg/ml F(ab′)$_2$ anti-IgM at 60 s; dark arrows shown 10 μM ionomycin administered at 270 s. All four genotypes were analyzed concurrently in each experiment. Results are representative of three independent experiments.

Discussion

The requirement for PS-mediated cleavage in activation of Notch family proteins predicted that inactivation of PS1 and PS2 in the B cell lineage would result in phenotypes overlapping with those associated with targeted deletion of Notch family members. Accordingly, we observed defective marginal zone and T2 B cell development in PS-deficient B cells, reminiscent of observations in Notch2-deficient and RBP-J-deficient B cells (27–29). However, the defects in signaling we have observed in PS-deficient B cells are likely to be independent of defects in Notch activation because both LPS-mediated proliferation and anti-IgM-mediated calcium flux were normal in B cells lacking RBP-J, a crucial intermediate implicated in Notch signaling (28). Taken together, our findings are consistent with a fundamental, unanticipated role for PS proteins in B cell signal transduction.

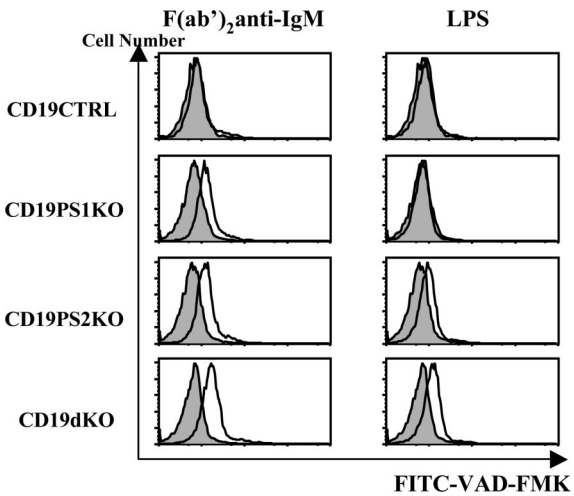

Fig. 5. Increased apoptosis after BCR or LPS stimulation of B cells lacking PS proteins. Flow cytometry histograms of fluorescence of the FITC-conjugated caspase inhibitor VAD-FMK at time 0 (gray shaded) and 5 h after treatment (unshaded) of purified control, PS1-deficient, PS2-deficient, and PS1/PS2-deficient splenic B cells with 3 μg/ml F(ab′)$_2$ anti-IgM (*Left*) and 12.5 μg/ml LPS (*Right*). Data presented reflect results from three independent experiments.

We also observed varying degrees of decreased proliferation and signal transduction in B cells lacking either PS1 or PS2. For example, proliferative responses to anti-IgM were significantly reduced relative to control for PS1- or PS2-deficient B cells; by contrast, in such single-deficient cells LPS-induced proliferation was reduced but relatively preserved compared with control. Although we note that these observations result from a substantial, but incomplete Cre recombinase-mediated deletion of PS1, these findings nonetheless suggest that the two mammalian PS proteins may have differential functions in mitogenic B cell proliferation. Notably, it appears that PS1 and PS2 have redundant functions downstream of LPS-mediated but not BCR-mediated proliferation. Whether the nonredundant functions of PS1 and PS2 downstream of BCR-induced proliferation reflect an epistatic relationship, complex formation, or parallel signaling pathways remains to be determined.

Our results are consistent with the notion that PSs have dual functions as I-CLiPs and as proteins critical for calcium-dependent signaling. Whether these functions are independent

or interrelated remains to be determined; however, it is worth noting that I-CLiP-deficient mutants of PS1 or PS2 were nonetheless able to complement the calcium flux defect in PS-deficient fibroblasts (5). Such fibroblasts had abnormally elevated calcium flux, which was rescued by ectopic PS expression, in contrast to the essential absence of intracellular calcium flux in response to anti-IgM we observed in PS-deficient B cells. Consequently, it is conceivable that PS function in calcium signaling may be distinct in different cell types. Notably, our observation of persistent decreases in intracellular calcium mobilization even to a calcium ionophore such as ionomycin also suggests a role for PS1 and/or PS2 as a potential component of the cellular calcium channel machinery mediating calcium flux in response to mitogenic signals in B cells. Our findings suggest that alterations in PS function, such as in the setting of pharmacologic inhibition of PS activity, could have consequences not only in the central nervous system but also for host defense as well.

Methods

Computational Analysis. ***CAGE analysis.*** We downloaded from the CAGE website (http://gerg01.gsc.riken.jp/expr_tree/mm5) cluster ID 64 among 70 clusters based on hierarchical clustering of 159,075 CAGE tag clusters across 23 tissue/cell type conditions. Cluster 64 contains contained 979 cluster tag IDs associated with the 5′ ends of genes that are expressed in immune cells such as macrophages both at baseline and upon activation with TLR ligands such as LPS and CpG. These 979 clusters mapped to 746 mouse genes with unique Entrez gene identifiers after considering presumed alternative 5′ promoters, cluster IDs not associated with a definitive protein-encoding gene, clusters mapping to known microRNAs such as miR-155 and miR-223 and other potential noncoding RNAs (SI Table 1).

Pathway/GO enrichment analysis. To examine pathways or biological processes in the immune CAGE promoter cluster (cluster 64) composed of 746 unique genes, we used the DAVID 2.0 program to compute enrichments of both the GO biological processes and KEGG pathways by using Fischer's exact probability with Bonferroni corrections, thereby identifying functional categories overrepresented in a gene list relative to the representation within the proteome of a given species (http://david.niaid.nih.gov/david/version2/index.htm) (19, 30).

Protein–protein interaction analysis. To derive protein–protein interaction networks on proteins annotated as either immune response (GO:0006955) and/or NF-κB cascade-related (GO:0007249), we used the BIND database (http://bond.unleashedinformatics.com) coupled with filtering algorithms to identify all interactions for human proteins with either of these GO ontologies and generated a base network of 341 nodes (proteins) and 261 connections (edges). We required that the experimental evidence for interaction be based on yeast two-hybrid screens, coimmunoprecipitation, affinity chromatography, or be part of part of mass spectrometry complexes (predicted complexes based on structural information were not included in the analysis). We used Cytoscape software to build the interaction map. Next, for each of the 341 nodes in the base network, the BIND data repository was also queried to identify protein interactions independent of GO ontology. The goal was to generate a first-order interaction map seeded with the immune response and NF-κB cascade network. We present the base map for simplicity purposes only (SI Table 5). A complete higher interaction map will presented elsewhere as part of a flexible analytical platform termed INPs that incorporates hundreds of datasets (C.G. and R.J.X., unpublished data).

Microarray analysis. To cross-validate that the 746 gene module (ID = 64) identified in the mouse CAGE promoter analysis was enriched in genes expressed in the immune system in a larger dataset, we analyzed the human orthologs (defined by reciprocal best hit) of these 746 genes across a compendium of human 79 tissues/cells profiled by microarray technology. The public version of the GNF human expression atlas version2 (20) was obtained from Novartis (http://wombat.gnf.org), including the primary.cel files, which used the U133a Affymetrix chip and a custom chip (GNF1H). The dataset contains the expression values of 33,690 probes reflecting normalization of each array to a set of 100 housekeeping genes common to both the U133a and custom GNF1H array. Subsequently, global median scaling across the arrays was performed, yielding expression values across samples for each probe set. The absent/present calls were analyzed, and probe sets with 100% absent calls across all 79 human tissues were not included in the analysis. The dataset was further filtered by requiring that a probe set have a threshold value >20 in at least one sample and a maximum–minimum expression value >100. A total of 28,852 reliable probes met the above filtering criteria. For each U133a probe set meeting the above criteria, its corresponding UniGene ID and LocusLink ID were identified based on the combined annotation tables provided at the http://wombat.gnf.org and NetAffyx websites (http://www.affymetrix.com). For the custom GNF1H chip, the mRNA/EST used to design the probe set was blasted against the exemplar sequences of the UniGene database (Build 116). Of the 28,852 probe sets, 26,789 mapped to 16,811 UniGene IDs. To represent the human expression profiles of mouse CAGE orthologs, hierarchical clustering with the centroid linkage method was performed by using DCHIP (31) with $1 - r$ as the distance metric, where r is the Pearson correlation coefficient, with relative expression levels displayed. From the murine 746 gene set from the CAGE coexpression cluster, we identified at least one probe for 652 of the 697 human orthologs that met our filtering criteria either the U133a or custom GNF1H arrays, as well as the default filtering criteria of DCHIP. Heat maps of hierarchical clustering of tissue expression and correlation values are based on a single-probe set per gene chosen at random so as to not bias the visual presentation. To ascertain whether any individual human orthologs of the 652 CAGE genes were enriched in the immune system in the normal tissue/cell compendium, we used the Wilcoxon rank sum test. To calculate the Wilcoxon statistic, we divided the 79 tissue/cell types into those of immune system origin ($n = 22$) and those that are not part of the immune system ($n = 57$), making two sample classes. The P values from the Wilcoxon test for each human ortholog probe of the mouse CAGE cluster were then calculated. Significant thresholds after multiple hypothesis testing were established by multiplying the Wilcoxon P value by the number of genes tested (Bonferroni correction). As shown in SI Fig. 7, the majority of CAGE genes not only clustered in immune cells but also were statistically enriched in expression compared with other tissues as denoted by a Wilcoxon score of $P < 0.05$ and identified by a tick mark on the left side of the heat map (SI Table 4).

Mice. Mice carrying a floxed *PS1* allele (25) and with germ line inactivation of PS2 (6) were crossed with CD19-Cre mice generously provided by K. Rajewsky (26). All mice were maintained under specific-pathogen free conditions. To facilitate analyses in experiments with littermate controls, CD19-Cre $PS1^{flox/+}$ $PS2^{+/-}$ mice were used as control mice, and CD19-Cre $PS1^{flox/flox}$ $PS2^{+/-}$, CD19-Cre $PS1^{flox/+}$ $PS2^{-/-}$, and CD19-Cre $PS1^{flox/flox}$ $PS2^{-/-}$ mice were analyzed to evaluate B cells lacking PS1 alone, PS2 alone, or both PS1 and PS2, respectively. Protocols for mouse experiments were approved by the Yale Animal Research Committee.

B Cell Preparation. Splenic B cells from 10- to 12-week-old mice were purified by negative sorting with magnetic beads and according to the manufacturer's instructions. (Invitrogen; Dynal Biotech). Such enrichment resulted in preparations of ≈80–90% $B220^+$ cells as analyzed by flow cytometry.

Flow Cytometry. RBC-depleted single-cell suspensions were stained with FITC-conjugated, anti-IgM (II/4), anti-CD21 (7G6), phycoerythrin (PE)-conjugated anti-CD23 (B3B4), anti-CD43 (S7) PE-Cy7-conjugated anti-IgM (R6–60.2), and allophycocyanin (APC)-conjugated anti-B220 (RA3–6B2) monoclonal antibodies. (BD PharMingen). Cell-associated fluorescence was analyzed with a FACSCalibur (BD Bioscience) instrument and FlowJo software (TreeStar). Numbers of MZB cells in the spleen were calculated from enumeration of $B220^+$-gated, $CD21^{hi}CD23^{lo}$ cells; follicular B from $CD23^+$-gated, $CD21^{lo}IgM^{lo}$; T1 $CD23^-$-gated, $CD21^{lo}IgM^{hi}$; and T2 $CD23^+$-gated, $CD21^{hi}IgM^{hi}$ cells.

Proliferation Assay. Splenic B cells isolated as described above were loaded with CFSE (Molecular Probes) in PBS to a final concentration of 2 μM, washed, and treated with anti-IgM $F(ab')_2$ (5 μg/ml) or LPS (20 μg/ml). The CFSE content of B220-gated cells was determined by flow cytometry after 4 days in culture.

Analysis of Calcium Mobilization. Splenocytes (2×10^6 /ml) were loaded with 1-[2-amino-5-(2,7-dichloro-6-hydroxy-3-oxo-9-xanthenyl)phenoxy]-2-(2-amino-5-methylphenoxy)ethane-*N*,*N*,*N*′,*N*′-tetraacetic acid, pentaacetoxymethyl ester (Fluo3-AM) (Molecular Probes) (final concentration 10 μM) at 37°C for 40 min and stained with APC-conjugated anti-B220 antibody. After washing, cells were resuspended in calcium-free PBS before treatment with 10 μg/ml $F(ab')_2$ anti-IgM. After 270 s, ionomycin (Sigma–Aldrich) was added to each sample (final concentration, 10 μM).

Phosphorylation Analysis. Splenocytes (2.5×10^6) were resuspended in 1 ml of PBS and preincubated at 37°C for 10 min. A control aliquot of 5×10^5 cells was removed, and the remaining cells were stimulated with 10 μg/ml $F(ab')_2$

anti-IgM or 20 μg/ml LPS. Aliquots of 5×10^5 cells were removed at 1, 5, and 15 min after stimulation, fixed, and permeabilized before the addition of anti-phosphospecific-Syk (I120–722) or anti-phosphospecific-p38 antibodies (clone 36) and APC-conjugated anti-B220 antibodies (all from PharMingen) for 1 h in the dark, followed by analysis by flow cytometry.

Apoptosis Assay. Purified splenic B cells were incubated at 1×10^6 cells per ml and treated with either 3 μg/ml $F(ab')_2$ anti-IgM (Jackson ImmunoResearch) or 12.5 μg/ml LPS (Sigma) for 5 h. Caspase activation reflecting apoptosis was quantified by using a fluorescein-labeled VAD-FMK reagent (CaspGLOW; BioVision Research Products) and gating on $B220^+$ cells.

Note Added in Proof. Recently, Laky and Fowlkes (32) employed a CD4-Cre transgene to evaluate presenilin-deficient T lineage cells and observed alterations in T cell development and impaired T cell receptor signaling.

ACKNOWLEDGMENTS. We thank Klaus Rajewsky (CBR Institute for Biomedical Research, Harvard Medical School) for CD19-Cre mice; Karen Duff (Columbia University, New York) for additional strains of *PS2*$^{-/-}$ mice; and Ruslan Medzhitov, Brian Seed, Mark Daly, and Daniel Podolsky for helpful comments on the manuscript. This work was supported by National Institutes of Health Grants T32 AI007517 (to T.Y.), NS41783 (to J.S.), NS40039 (to H.Z.), and AI062773 (to R.J.X.). A.C.S. was a Brookdale Foundation National Fellow and T. Franklin Williams Scholar.

1. Vetrivel KS, Zhang YW, Xu H, Thinakaran G (2006) *Mol Neurodegener* 1:4.
2. Selkoe D, Kopan R (2003) *Annu Rev Neurosci* 26:565–597.
3. LaFerla FM (2002) *Nat Rev Neurosci* 3:862–872.
4. Mattson MP, Chan SL, Camandola S (2001) *Bioessays* 23:733–744.
5. Tu H, Nelson O, Bezprozvanny A, Wang Z, Lee SF, Hao YH, Serneels L, De Strooper B, Yu G, Bezprozvanny I (2006) *Cell* 126:981–993.
6. Donoviel DB, Hadjantonakis AK, Ikeda M, Zheng H, Hyslop PS, Bernstein A (1999) *Genes Dev* 13:2801–2810.
7. Shen J, Bronson RT, Chen DF, Xia W, Selkoe DJ, Tonegawa S (1997) *Cell* 89:629–639.
8. Wong PC, Zheng H, Chen H, Becher MW, Sirinathsinghji DJ, Trumbauer ME, Chen HY, Price DL, Van der Ploeg LH, Sisodia SS (1997) *Nature* 387:288–292.
9. Qyang Y, Chambers SM, Wang P, Xia X, Chen X, Goodell MA, Zheng H (2004) *Biochemistry* 43:5352–5359.
10. Tournoy J, Bossuyt X, Snellinx A, Regent M, Garmyn M, Serneels L, Saftig P, Craessaerts K, De Strooper B, Hartmann D (2004) *Hum Mol Genet* 13:1321–1331.
11. Mootha VK, Lindgren CM, Eriksson KF, Subramanian A, Sihag S, Lehar J, Puigserver P, Carlsson E, Ridderstrale M, Laurila E, *et al*. (2003) *Nat Genet* 34:267–273.
12. Tomlins SA, Mehra R, Rhodes DR, Cao X, Wang L, Dhanasekaran SM, Kalyana-Sundaram S, Wei JT, Rubin MA, Pienta KJ, *et al*. (2007) *Nat Genet* 39:41–51.
13. Levine DM, Haynor DR, Castle JC, Stepaniants SB, Pellegrini M, Mao M, Johnson JM (2006) *Genome Biol* 7:R93.
14. Hyatt G, Melamed R, Park R, Seguritan R, Laplace C, Poirot L, Zucchelli S, Obst R, Matos M, Venanzi E, *et al*. (2006) *Nat Immunol* 7:686–691.
15. Carninci P, Sandelin A, Lenhard B, Katayama S, Shimokawa K, Ponjavic J, Semple CA, Taylor MS, Engstrom PG, Frith MC, *et al*. (2006) *Nat Genet* 38:626–635.
16. Stuart JM, Segal E, Koller D, Kim SK (2003) *Science* 302:249–255.
17. Mootha VK, Lepage P, Miller K, Bunkenborg J, Reich M, Hjerrild M, Delmonte T, Villeneuve A, Sladek R, Xu F, *et al*. (2003) *Proc Natl Acad Sci USA* 100:605–610.
18. Giallourakis C, Cao Z, Green T, Wachtel H, Xie X, Lopez-Illasaca M, Daly M, Rioux J, Xavier R (2006) *Genome Res* 16:1056–1072.
19. Hosack DA, Dennis G, Jr, Sherman BT, Lane HC, Lempicki RA (2003) *Genome Biol* 4:R70.
20. Su AI, Wiltshire T, Batalov S, Lapp H, Ching KA, Block D, Zhang J, Soden R, Hayakawa M, Kreiman G, *et al*. (2004) *Proc Natl Acad Sci USA* 101:6062–6067.
21. Li SH, Lam S, Cheng AL, Li XJ (2000) *Hum Mol Genet* 9:2859–2867.
22. Ona VO, Li M, Vonsattel JP, Andrews LJ, Khan SQ, Chung WM, Frey AS, Menon AS, Li XJ, Stieg PE, *et al*. (1999) *Nature* 399:263–267.
23. Khoshnan A, Ko J, Watkin EE, Paige LA, Reinhart PH, Patterson PH (2004) *J Neurosci* 24:7999–8008.
24. Ogura Y, Sutterwala FS, Flavell RA (2006) *Cell* 126:659–662.
25. Feng R, Rampon C, Tang YP, Shrom D, Jin J, Kyin M, Sopher B, Miller MW, Ware CB, Martin GM, *et al*. (2001) *Neuron* 32:911–926.
26. Rickert RC, Roes J, Rajewsky K (1997) *Nucleic Acids Res* 25:1317–1318.
27. Saito T, Chiba S, Ichikawa M, Kunisato A, Asai T, Shimizu K, Yamaguchi T, Yamamoto G, Seo S, Kumano K, *et al*. (2003) *Immunity* 18:675–685.
28. Tanigaki K, Han H, Yamamoto N, Tashiro K, Ikegawa M, Kuroda K, Suzuki A, Nakano T, Honjo T (2002) *Nat Immunol* 3:443–450.
29. Witt CM, Won WJ, Hurez V, Klug CA (2003) *J Immunol* 171:2783–2788.
30. Dennis G, Jr, Sherman BT, Hosack DA, Yang J, Gao W, Lane HC, Lempicki RA (2003) *Genome Biol* 4:P3.
31. Schadt EE, Li C, Ellis B, Wong WH (2001) *J Cell Biochem Suppl* 37:120–125.
32. Laky K, Fowlkes BJ (2007) *J Exp Med* 204:2115–2129.